Available online at www.sciencedirect.com
SCIENCE DIRECT®
Dyes and Pigments 58 (2003) 27–35
DYES and PIGMENTS
www.elsevier.com/locate/dyepig

Antimicrobial cationic dyes: part 1: synthesis and characterization

Minghua Ma, Yuyu Sun, Gang Sun*

Division of Textiles and Clothing, University of California, Davis, CA 95616, USA

Received 7 October 2002; received in revised form 27 November 2002; accepted 30 January 2003

Abstract

As an attempt to combine dyeing and functional finishing in one process, novel antimicrobial cationic dyes were prepared by reacting *N,N*-dimethylbutylamine, *N,N*-dimethyloctylamine and *N,N*-dimethyldodecylamine with anthraquinone derivatives, respectively. The structures of the dyes were fully characterized by using FTIR, ^{1}H-NMR and ^{13}C-NMR analysis. Their color characteristics were studied in terms of λ_{max} and ε_{max} in aqueous solution. The antimicrobial efficacy of these dyes was evaluated by using a minimum inhibitory concentration (MIC) as an indicator. All of the synthesized dyes showed antimicrobial activities against both Gram-positive and Gram-negative bacteria, but in different levels depending on their structures. The structure–property relationships of the dyes were further discussed.

Keywords: Synthesis; Characterization; Antimicrobial; Quaternary ammonium salts; Cationic dyes; Anthraquinones

1. Introduction

Textile dyeing and functional finishing are two necessary but traditionally separated processes employed in textile treatments. Textile dyeing and finishing necessitate repeated wet treatments and drying, and thus consume large quantities of energy and produce large amounts of wastewater. Simultaneous dyeing and finishing in one bath could obviously reduce both the costs of production and waste. Recent work has demonstrated that the combination of these two processes is feasible [1–4]. However, the different treatment conditions required for textile dyeing and functional finishing generally limit the application of such processes to the mixing of colorants and finishing agents in a one-step treatment. As an alternative approach, if a functional agent was chemically incorporated into a dye without significantly affecting its dyeing properties, the textile dyeing and finishing could be unified into one process (Fig. 1). The design of a functional dye becomes the key to fulfill this goal.

A functional dye or colorant is not a completely novel concept. Generally speaking, dyes and colorants are compounds whose electronic structures can absorb electromagnetic radiation in visible range (380–780 nm). Additional properties other than color can be defined as functions. Based on this definition, infrared dyes, laser dyes and voltage

* Corresponding author. Tel.: +1-530-752-0840; fax: +1-530-752-7584.
E-mail address: gysun@ucdavis.edu (G. Sun).

0143-7208/03/$ - see front matter
doi:10.1016/S0143-7208(03)00025-1

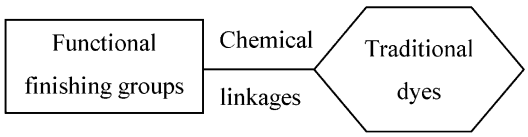

Fig. 1. The structure of functional dyes.

sensitive dyes fall within the category of functional dyes [5]. However, our concept of a functional dye is more specifically associated with the traditional functions that textile fabrics or clothing materials should possess. These functions can include, but are not limited to, the following properties such as water repellent, fire-resistant, antimicrobial, anti-UV, and anti-chemical finishes.

In an attempt to prepare a functional dye, a series of antimicrobial dyes were designed and synthesized by incorporating biocidal quaternary ammonium salts (QAS) into aminoanthraquinioid dyes (see Fig. 2). QAS inactivate microorganisms by disturbing their cytoplasmic membrane and have been widely used as surface disinfectants and antimicrobial finishing agents in textiles [3,4,6]. Meanwhile, anthraquinioid structures are excellent chromophores and have been much employed in dyes. Since quaternary ammonium structures carry a positive charge on its nitrogen atom, our aim was to prepare an antimicrobial dye of similar structure to that of a traditional cationic dye and, therefore, to achieve simultaneous dyeing and functional finishing using a cationic dyeing process. This paper focuses on the synthesis and characterization of these novel cationic dyes. The antimicrobial ability of these dyes was also evaluated against Gram-positive and Gram-negative bacteria. The dyeing performance of the dyes on acrylic and other related fibers will be discussed in following parts of this paper.

2. Experimental

2.1. Materials and instrumentation

1,4-Diaminoanthraquinone (90%, Aldrich) was purified by repeated crystallization from acetone. 1-aminoanthraquinone (97%, Aldrich), chloroacetyl chloride (98%, Acros), *N,N*-dimethylbutylamine (99%, Aldrich), *N,N*-dimethyloctylamine (97%, Acros), *N,N*-dimethyldodecylamine (95%, Acros) were used as received.

The melting points of the samples were measured using a Shimadzu DSC-50 instrument at a heating rate of 10 °C min^{-1} under a N_2 atmosphere. FTIR spectra were taken on a Nicolet Magana IR-560 spectrometer using KBr pellets. The samples were made thin enough to ensure that the Beer–Lambert law was obeyed. ^{1}H-NMR and ^{13}C-NMR spectra were recorded on a Varian Mercury 300 spectrometer. Electronic absorption spectra were recorded on a Hitachi U-2000 spectrophotometer.

2.2. Synthesis

The first step of the synthesis was the acetylation of the α-amino anthraquinioid (AQ) group using chloroacetyl chloride according to a method reported elsewhere [7]. The second step was a quateranization of the primary chloride with different tertiary amines. The synthetic procedures

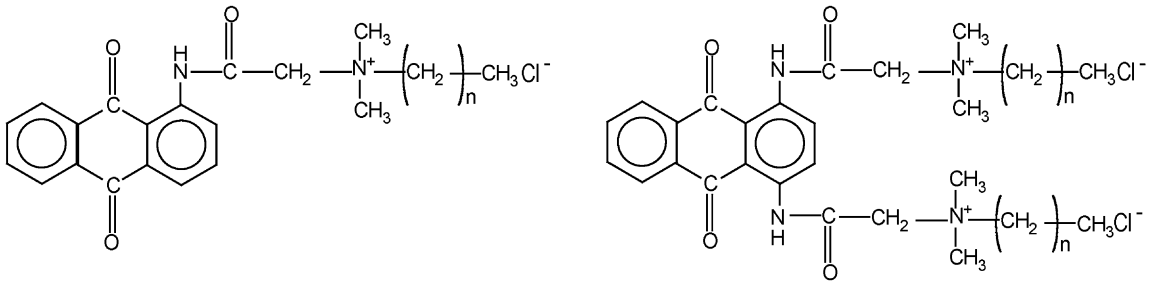

Fig. 2. The structures of antimicrobial cationic dyes ($n = 3, 7, 11$).

are outlined in Fig. 3; the list of compounds prepared is presented in Table 1.

2.2.1. Synthesis of I_c

0.01 mol 1-aminoanthraquinone (I_a) in 30 ml dimethylacetamide was cooled to 0 °C, and 5 ml (0.06 mol) chloroacetyl chloride in 150 ml of chloroform was slowly added with vigorous stirring. The reaction mixture was further stirred for 1 h at room temperature and the solvent was evaporated under vacuum. The product was precipitated by addition of ethyl ether. The crude product I_b (1-chloroacetamido-9,10-anthracenedione) was purified by recrystallization from *N,N*-dimethylformamide (DMF) with a yield of 78%. After acetylation, a suspension of 0.01 mol I_b in 200 ml DMF, together with 0.1 mol *N,N*-dimethylbutylamine, was heated at 95 °C for 3 h. After

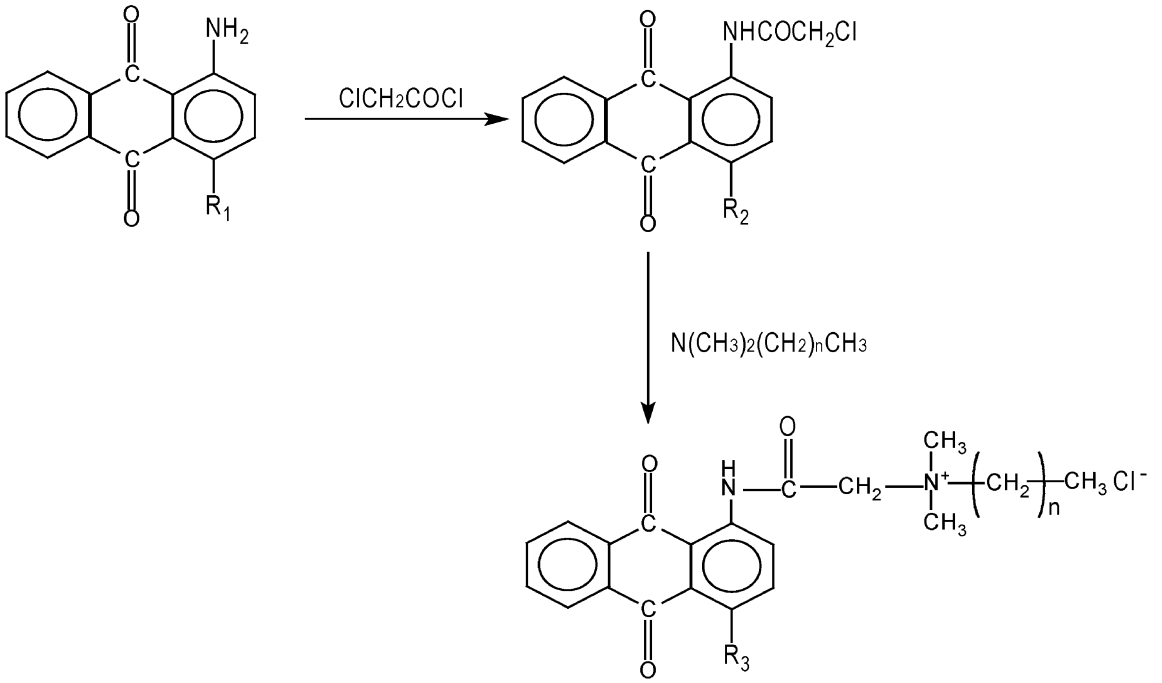

Fig. 3. The synthetic procedures for cationic dyes ($n = 3, 7, 11$).

Table 1
List of compounds involved in the synthesis

Compound	R_1	R_2	R_3
I_a	H	–	–
I_b	–	H	–
I_c	–	–	H
I_d	–	–	H
I_e	–	–	H
II_a	NH_2	–	–
II_b	–	$NHCOCH_2Cl$	–
II_c	–	–	$NHCOCH_2N^+(CH_3)_2(CH_2)_3CH_3Cl^-$
II_d	–	–	$NHCOCH_2N^+(CH_3)_2(CH_2)_7CH_3Cl^-$
II_e	–	–	$NHCOCH_2N^+(CH_3)_2(CH_2)_{11}CH_3Cl^-$

removing DMF under reduced pressure, the product was purified from ethyl ether–ethyl alcohol solvent mixture. Yield 65%, melting point: 219 °C. IR spectra data (KBr): $\nu_{-NH-CO-} = 1700\ cm^{-1}$. ^{1}H-NMR spectra data ($CDCl_3$, δ): 12.597 (singlet, 1H, –NH–CO–); 8.663∼8.696, 8.102∼8.159, 7.958∼7.987, 7.573∼7.721 (multiplet, multiplet, multiplet, multiplet, 7H, protons attached to C_2,C_3, C_4, C_5, C_6, C_7, C_8); 5.578 (singlet, 2H, –CO–CH_2–$N^+(CH_3)_2C_4H_9$), 3.914∼3.970 (broad multiplet, 2H, –$N^+(CH_3)_2$–CH_2–C_3H_7), 3.757 (singlet, 6H, –$N^+(CH_3)_2$–CH_2–C_3H_7), 1.857 (broad multiplet, 2H, –$N^+(CH_3)_2$–CH_2–CH_2–C_2H_5), 1.438∼1.510 (multiplet, 2H, –$N^+(CH_3)_2$–CH_2–CH2–$CH2$–CH_3), 0.997∼1.046 (triplet, 3H, –$N^+(CH_3)_2$–CH_2–CH_2–CH_2–CH_3).

2.2.2. Synthesis of I_d

I_d was prepared by using the same procedure in preparation of I_c. Yield: 62%, melting point: 205 °C. IR spectra data (KBr): $\nu_{-NH-CO-} = 1705\ cm^{-1}$. ^{1}H-NMR spectra data ($CDCl_3$, δ): 12.552 (singlet, 1H, –NH–CO–); 8.612∼8.636, 7.990∼8.091, 7.863∼7.889, 7.506∼7.668 (multiplet, multiplet, multiplet, multiplet, 7H, protons attached to C_2,C_3, C_4, C_5, C_6, C_7, C_8); 5.683 (singlet, 2H, –CO–CH_2–$N^+(CH_3)_2C_8H_{17}$), 3.905∼3.980 (broad multiplet, 2H, –$N^+(CH_3)_2$–CH_2–C_7H_{15}), 3.778 (singlet, 6H, –$N^+(CH_3)_2$–CH_2–C_7H_{15}), 1.827 (broad peak, 2H, –$N^+(CH_3)_2$–CH_2–CH_2–C_6H_{13}), 1.383, 1.251 (broad peaks, 10H, –$N^+(CH_3)_2$–CH_2–CH_2–$(CH_2)_5$–CH_3), 0.831∼0.853 (triplet, 3H, –$N^+(CH_3)_2$–CH_2–CH_2–$(CH_2)_5$–CH_3).

2.2.3. Synthesis of I_e

By following similar procedures, I_e was also prepared. Yield: 65%, melting point: 206 °C. IR spectra data (KBr): $\nu_{-NH-CO-} = 1705\ cm^{-1}$. ^{1}H-NMR spectra data ($CDCl_3$, δ): 12.552 (singlet, 1H, –NH–CO–); 8.577∼8.606, 7.975∼8.065, 7.839∼7.864, 7.454∼7.664 (doublet, multiplet, doublet, multiplet, 7H, protons attached to C_2, C_3, C_4, C_5, C_6, C_7, C_8); 5.648 (singlet, 2H, –CO–CH_2–$N^+(CH_3)_2C_{12}H_{25}$), 3.905∼3.980 (broad multiplet, 2H, –$N^+(CH_3)_2$–CH_2–$C_{11}H_{23}$), 3.769 (singlet, 6H, –$N^+(CH_3)_2$–CH_2–$C_{11}H_{23}$), 1.857 (broad peak, 2H, –$N^+(CH_3)_2$–CH_2–CH_2–$C_{10}H_{21}$), 1.340, 1.191 (broad peaks, 18H, –$N^+(CH_3)_2$–CH_2–CH_2–$(CH_2)_9$–CH_3), 0.829 (triplet, 3H, –$N^+(CH_3)_2$–CH_2–CH_2–$(CH_2)_9$–CH_3).

2.2.4. Synthesis of II_c

0.01 mol of 1,4-diaminoanthraquinone (II_a) in 30 ml dimethylacetamide at 0 °C was reacted with 0.12 mol chloroacetyl chloride in 300 ml chloroform. The acetylation reaction also had a yield of 76%. A suspension of 0.01 mol 1,4-bis(chloroacetamido)-9,10-anthracenedione (II_b) in 300 ml DMF, together with 0.2 mol N,N-dimethylbutylamine, was heated at 95 °C for 3 h. The final product was purified by ethyl ether–ethyl alcohol solvent mixture. Yield: 62%, melting point: 221 °C. IR spectra data (KBr): $\nu_{-NH-CO-} = 1705\ cm^{-1}$. ^{1}H-NMR spectra data ($CDCl_3$, δ): 12.611 (singlet, 2H, –NH–CO–); 8.021, 7.959∼7.989, 7.671∼7.700 (singlet, multiplet, multiplet, 6H, protons attached to C_2, C_3, C_5, C_6, C_7, C_8); 5.962 (singlet, 4H, –CO–CH_2–$N^+(CH_3)_2C_4H_9$), 3.972∼4.029 (broad multiplet, 4H, –$N^+(CH_3)_2$–CH_2–C_3H_7), 3.790 (singlet, 12H, –$N^+(CH_3)_2$–CH_2–C_3H_7), 1.916 (broad peak, 4H, –$N^+(CH_3)_2$–CH_2–CH_2–C_2H_5), 1.478∼1.528, 1.191 (multiplet, 4H, –$N^+(CH_3)_2$–CH_2–CH_2–CH_2–CH_3), 1.014∼1.063 (Triplet, 6H, –$N^+(CH_3)_2$–CH_2–CH_2–CH_2–CH_3).

2.2.5. Synthesis of II_d

II_d was also prepared by using the procedure described for the preparation of II_c. Yield: 65%, melting point: 235 °C. IR spectra data (KBr): $\nu_{-NH-CO-} = 1706\ cm^{-1}$. ^{1}H-NMR spectra data ($CDCl_3$, δ): 12.545 (singlet, 2H, –NH–CO–); 7.939∼7.969, 7.648∼7.678 (triplet, multiplet, 6H, protons attached to C_2, C_3, C_5, C_6, C_7, C_8); 5.927 (singlet, 4H, –CO–CH_2–$N^+(CH_3)_2C_8H_{17}$), 3.986 (broad multiplet, 4H, –$N^+(CH_3)_2$–CH_2–C_7H_{15}), 3.778 (singlet, 12H, –$N^+(CH_3)_2$–CH_2–C_7H_{15}), 1.892 (broad peak, 4H, –$N^+(CH_3)_2$–CH_2–CH_2–C_6H_{13}), 1.396, 1.269 (broad peaks, 20H, –$N^+(CH_3)_2$–CH_2–CH_2–$(CH_2)_5$–CH_3), 0.845∼0.968 (triplet, 6H, –$N^+(CH_3)_2$–CH_2–CH_2–$(CH_2)_5$–CH_3).

2.2.6. Synthesis of II_e

II_e was prepared in the similar procedure as preparing II_c. Yield: 60%, melting point: 234 °C. IR spectra data (KBr): $\nu_{-NH-CO-} = 1708\ cm^{-1}$.

^{1}H-NMR spectra data ($CDCl_3$, δ): 12.434 (singlet, 2H, –NH–CO–); 7.896, 7.865, 7.649 (multiplet, singlet, multiplet, 6H, protons attached to C_2, C_3, C_5, C_6, C_7, C_8); 5.846 (singlet, 4H, –CO–CH_2–$N^+(CH_3)_2C_{12}H_{25}$), 3.982 (broad multiplet, 4H, –$N^+(CH_3)_2$–CH_2–$C_{11}H_{23}$), 3.754 (singlet, 12H, –$N^+(CH_3)_2$–CH_2–$C_{11}H_{23}$), 1.899 (broad peak, 4H, –$N^+(CH_3)_2$–CH_2–CH_2–$C_{10}H_{21}$), 1.391, 1.243 (broad peaks, 36H, –$N^+(CH_3)_2$–CH_2–CH_2–$(CH_2)_9$–CH_3), 0.866 (Triplet, 6H, –$N^+(CH_3)_2$–CH_2–CH_2–$(CH_2)_9$–CH_3).

2.3. Antimicrobial assessment

The antimicrobial properties of the functional dyes were evaluated using a minimum inhibitory concentration (MIC), this being the concentration at which no growth of bacteria was observed following such a procedure [8]. 1 ml of an aqueous suspension containing 10^6–10^7 colony-forming units (CFU)/mL of *Staphylococcus aureus* (Gram-positive) or *Escherichia coli* (Gram-negative) were placed into 9 ml aqueous solutions with different dye concentrations. After 24 h, a 100 μl aliquot of the resultant solution was serially diluted by sterilized distilled water to 100 ml. 100 μl of the dilution were placed onto a nutrient agar plate and incubated at 37 °C for 24 h. The same procedure was applied to a distilled water solution without dyes as a control.

3. Results and discussion

3.1. Characterization

The FT-IR spectra of I_a–I_e are shown in Fig. 4. I_a shows absorbance bands at 3416, 3298, and 1665 cm^{-1}, which can be attributed to the hydrogen-bonded primary amines, and the C=O stretching band of the anthraquinone structures, respectively, in agreement with the literature data [9]. However, in the region of 3200–3500 cm^{-1}, I_b–I_e only show one band at about 3430 cm^{-1}, strongly indicating that the primary amine in I_a has been transformed into amides. Besides, in the spectra of I_b–I_e, a new peak centered around 1690–1700 cm^{-1} can be observed, which is most likely caused by the carbonyl groups of the amide structures. It is also interesting to note that with the increase of alkane chain length in quaternary ammonium salts, the intensity of the alkane absorption bands (2800–3000 cm^{-1}) also gradually increased (see Fig. 4, I_c–I_e for details). Similar phenomena was observed in the FT-IR spectra of II_a–II_e.

The chemical structures of the synthesized dyes were further confirmed by ^{1}H- and ^{13}C-NMR analysis. As an example, Fig. 5 shows the ^{1}H spectrum of I_d. The multiple peaks in the region of δ 7.506∼8.612 ppm are assigned to aromatic protons [9]. Additionally, several characteristic peaks of the dyes can also be found. For example, the peak centered at 12.552 ppm should be the amide proton (H_a), and the signal at 5.683 ppm can be attributed to H_b (see Fig. 5 for details). In the ^{13}C spectrum of I_d (Fig. 6), the peaks at 186.312 and 181.847 ppm are assigned to the two carbonyl carbons in the anthraquinone structure, respectively. The amide carbon appears at 163.984 ppm. The 12 peaks in the range of 100∼140 ppm are caused by the aromatic carbons, and the 10 peaks within 10∼70 ppm are corresponding to the 11 alkyl carbons, which locate in ten different chemical environments. All these findings strongly suggest that new cationic dyes can be readily synthesized following the reactions shown in Fig. 3.

3.2. Absorption spectra

Adsorption spectra of the synthesized dyes are shown in Fig. 7. The corresponding λ_{max} and molar absorptivity (ε_{max}) are listed in Table 2. As

Table 2
Spectral data and MIC of the synthesized cationic dyes (in water)

	I_c	I_d	I_e	II_c	II_d	II_e
λ_{max} (nm)	379	379	379	431	436	449
ε_{max} (L mol^{-1} cm^{-1})	1895	1880	1626	2043	2001	1977
MIC *S. aureus* (ppm)	>800	80	20	800	60	20
MIC *E. coli* (ppm)	>800	50	20	600	20	20

MIC is expressed in ppm of dyes.

expected, the di-substituted anthraquinioid dyes showed greater bathochromicity compared to the mono-substituted ones, in good agreement with theoretical predictions [10]. Furthermore, with the increase of alkyl chain length in the quaternary ammonium salts, mono-substituted dyes have the same λ_{max} at 379 nm while di-substituted ones show a bathochromic shift. We believe that this phenomenon may be related to the increased steric hindrance caused by the longer alkyl chains in the di-substituted QAS. In aqueous solutions, three types of hydrogen-bonding may be formed for these dyes, i.e., intramolecular hydrogen-bonding, intermolecular hydrogen-bonding as well as hydrogen-bonding with water molecules, as shown in Fig. 8. It has been reported that intramolecular hydrogen-bonding can lead to a bathochromic shift through a combination of two effects namely: (a) enhancing the electron-donating ability of the amide group and the electron-withdrawing ability of the carbonyl group, and (b) holding the groups in a planar conformation [10]. However, the

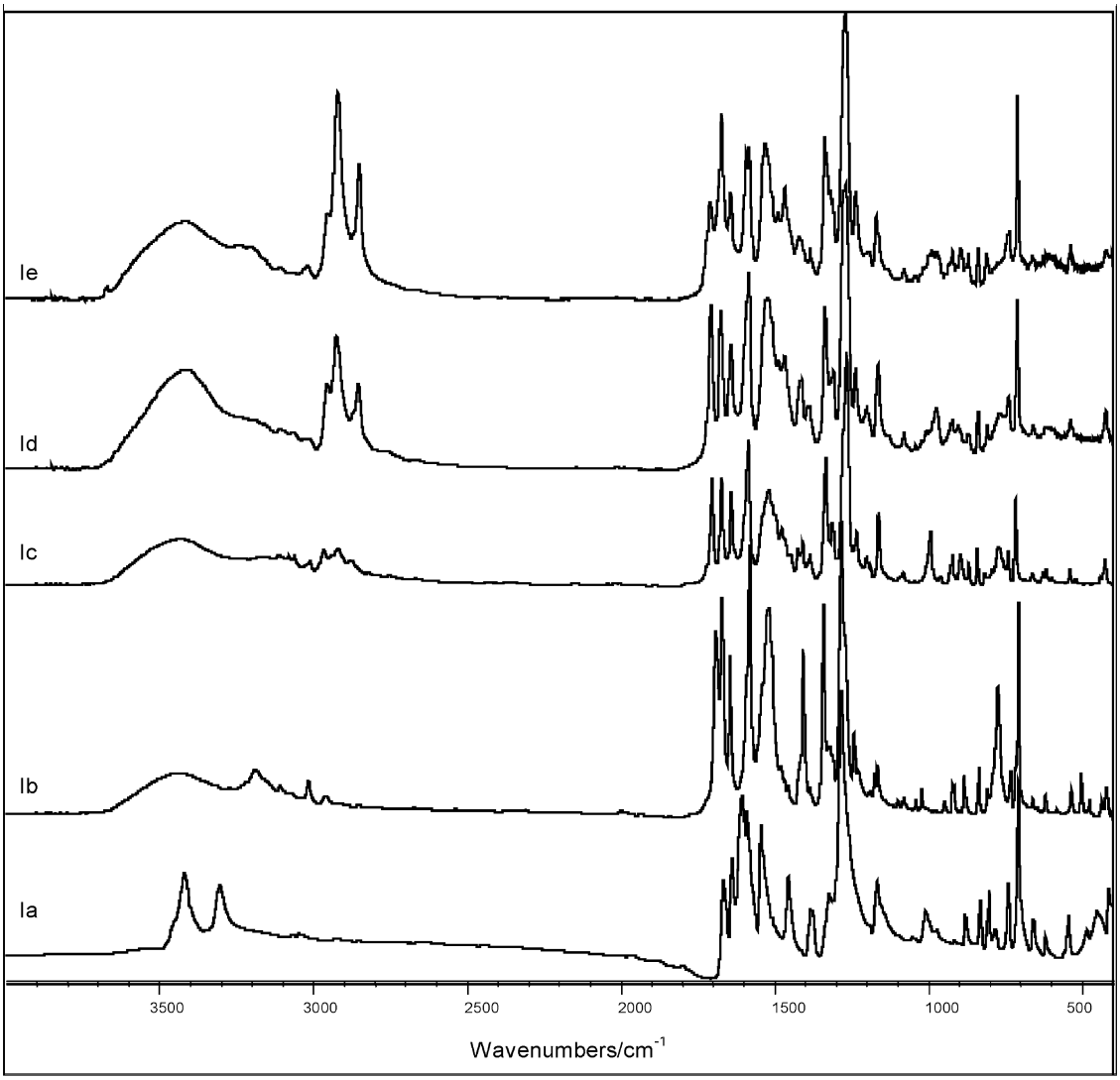

Fig. 4. The FT-IR spectra of I_a–I_e.

formation of the other two types of hydrogen-bonding has no such effect. In the case of the di-substituted AQ dyes, with the increase of the alkyl chain length in the QAS, the steric hindrance is increased, which may also increase the relative amount of intramolecular hydrogen-bonding but decrease the proportion of the other two hydrogen-bondings. Therefore, with increasing QAS chain length, greater bathochromicity was observed in the di-substituted dyes. However, this steric effect was not obvious in the mono-substituted dyes, indicating that with the increase of the alkyl chain length, the three types of hydrogen-bonding in this system probably did not undergo a proportional change as significantly as in II_c–II_e.

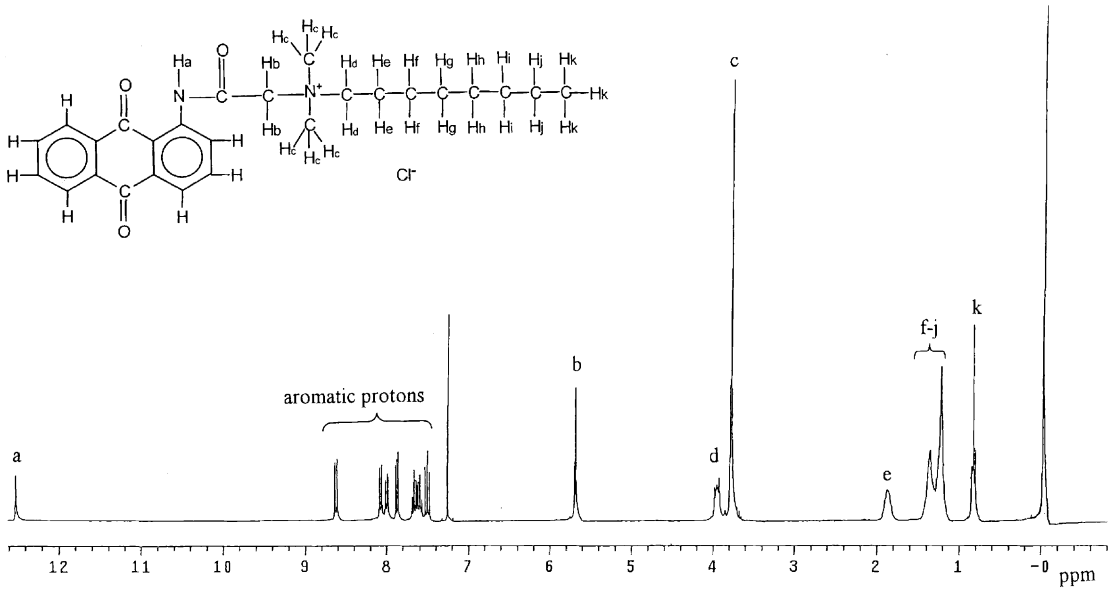

Fig. 5. The ^{1}H-NMR spectrum of I_d.

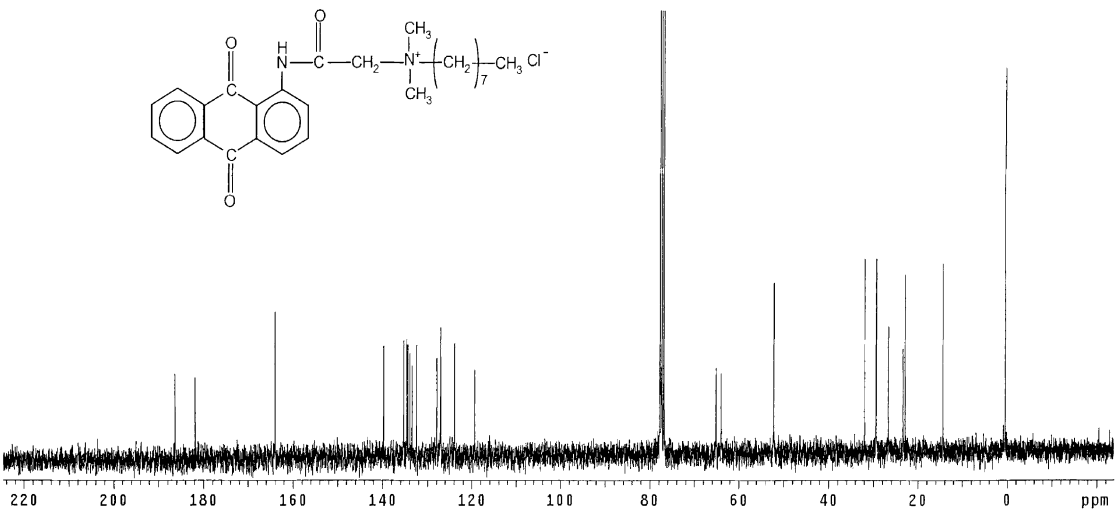

Fig. 6. The ^{13}C-NMR spectrum of I_d.

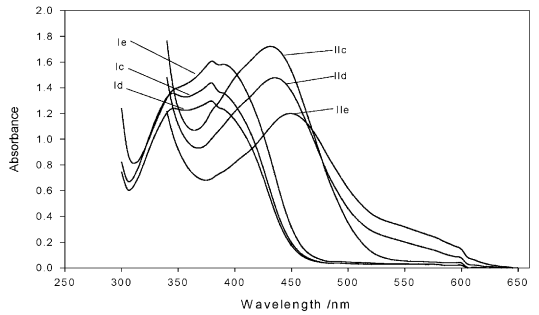

Fig. 7. UV–visible absorption spectra of the cationic dyes in water.

It is also worth noting that with the increase in alkyl chain length in QAS, all of the dyes showed a decrease in their ε_{max}. Usually, ϵ_{max} is a widely accepted measurement of tinctorial strength. However, assessing the tinctorial strength of dyes is quite difficult and, in some cases, controversial results could be obtained [10]. For example, an empirical rule states that for a given series of dyes, the tinctorial strength increases as the dyes become more bathochromic, whereas molecular orbital theory predicts that the tinctorial strength of dyes should decrease as λ_{max} increases. However, as a general

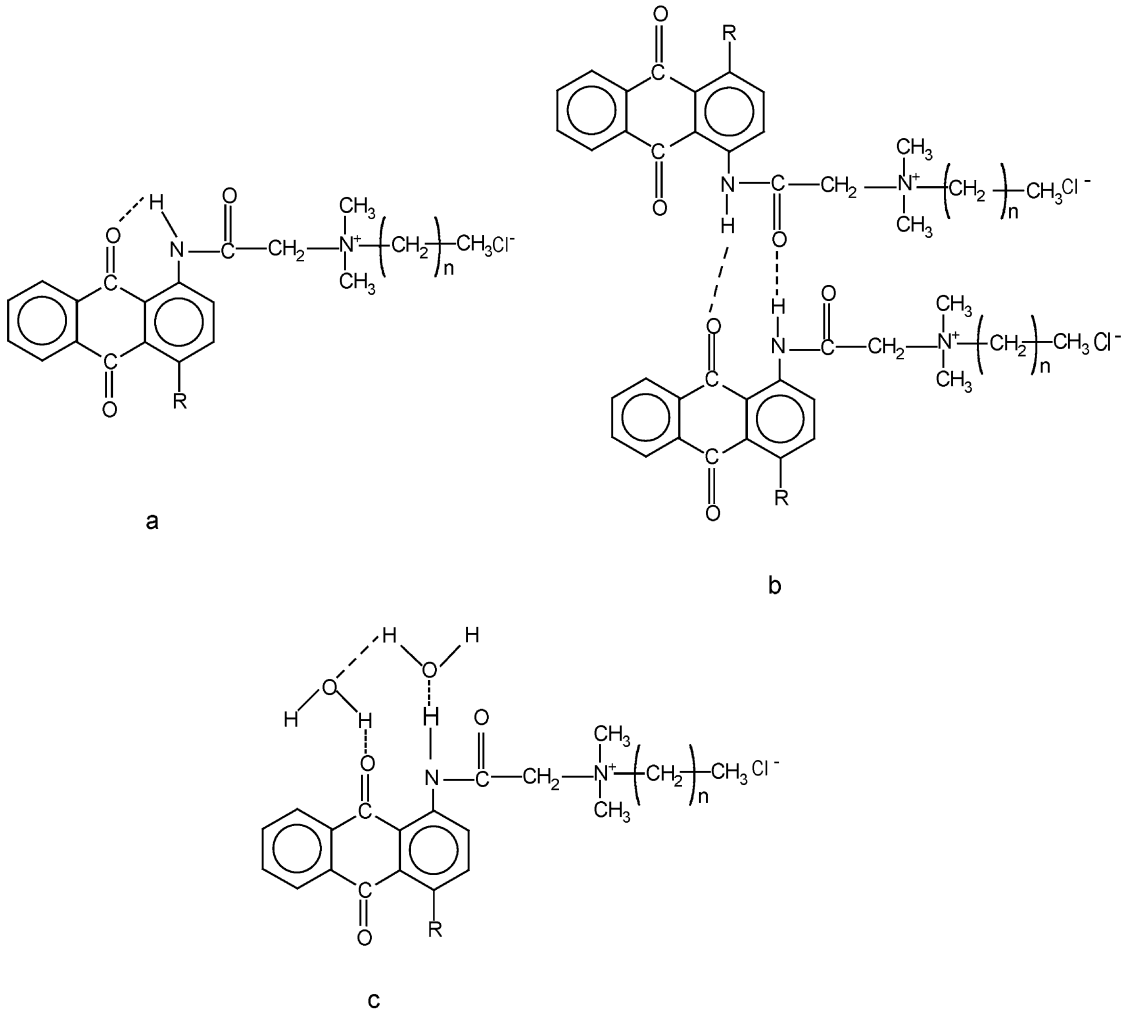

Fig. 8. Three types of hydrogen-bonding in aqueous solution: (a) intramolecular, (b) intermolecular, (c) with water molecules.

rule, steric hindrance always causes a reduction in tinctorial strength [10], which readily explains our experimental results, as shown in Table 2.

3.3. Antimicrobial efficacy

The MIC values of the cationic dyes against *S. aureus* and *E. coli* are listed in Table 2. All of the dyes showed biocidal properties against the bacteria, but to different degrees depending on their molecular structures. Generally speaking, with the increase of alkyl chain length in the QAS, the compounds exhibited higher antimicrobial activities. For example, I_c provided no effect even when a concentration higher than 800 ppm was used, and II_c also needed 500 ppm to achieve effective inactivation. However, I_d, I_e, II_d and II_e could provide a total kill of 10^6–10^7 CFU/mL of *S. aureus* or *E. coli* at a concentration as low as 100 ppm. These findings agree well with other reports, which demonstrated that if the alkyl chain of QAS contained less than eight carbons, they would only show weak antibacterial activities [11–13]. Besides, as expected, due to their higher quaternary ammonium salt content, the di-substituted dyes displayed higher antimicrobial activities than mono-substituted dyes.

It is also interesting to note that the dyes generally showed better antimicrobial efficacy against *E. coli* than *S. aureus*. These observations may be due to structural differences between the bacteria. For Gram-positive bacteria, the main component of the cell walls is a rigid network composed of three macromolecular concentric shells, while Gram-negative bacteria have a network that is only one molecule thick, together with up to 25% (mass) of lipoprotein and lipopolysaccharide [14]. Therefore, Gram-positive bacteria show greater resistance to mechanical rupture than Gram-negative cells. For example, Gram-positive bacteria can resist as high as 30 atmospheres of internal osmotic pressure; while for Gram-negative bacteria, the highest recorded internal osmotic pressure is only 8 atmospheres [14]. Since QAS damage the membrane through mechanical disruption, it is not surprising to find that the functional dyes showed stronger antimicrobial activities against Gram-negative cells (*E. coli*).

4. Conclusions

Novel antimicrobial cationic dyes were synthesized in good yield by incorporating quaternary ammonium salt moieties into aminoanthraquinioid dyes. It was found that the di-substituted dyes were of greater bathochromicity than mono-substituted dyes. An increase in the alkyl chain length in QAS lowered the ε_{max} of the dyes. All dyes exhibited antimicrobial efficacy against *S. aureus* and *E. coli,* with di-substituted dyes usually showing higher activitiy. It was also found that the alkyl chain length in QAS played an important role in antimicrobial functions. Lower than eight carbons in the QAS alkyl chain led to very low antimicrobial activities. In addition, the antimicrobial dyes provided higher antibacterial efficacy against Gram-negative bacteria than Gram-positive bacteria, which could be due to the structural differences between bacteria.

Acknowledgements

This research was supported by a CAREER Award from US National Science Foundation (DMI 9733981) and was financially sponsored by Vanson-HaloSource Inc. (Redmond, WA).

References

[1] Lewis DM, Broadlent PJ. J Soc Dyer Colorist 1997;113:159.
[2] Chol H-M, Srinivasan M, Morris NM. J Appl Polym Sci 1994;54:2107.
[3] Kim Y, Sun G. Textile Res J 2000;70(8):728.
[4] Kim Y, Sun G. Textile Res J 2001;71(4):318.
[5] Griffiths J. Chimia 1991;45:304.
[6] Latlief MA, Goldsmith MT, Friedl JL, Stuart LS. J Pediatrics 1951;39:730.
[7] Martelli S, Dzieduszycka M, Stefanska B, Bontemps-Gracz M, Borowski E. J Med Chem 1988;31(10):1956.
[8] Kaminski JJ, Hyycke MM, Selk SH, Bodor N, Higuchi T. J Pharm Sci 1976;65(12):1737.
[9] Silverstein RM, Webster FX. Spectrometric identification of organic compounds. New York: John Wiley & Sons; 1998.
[10] Gordon PF, Gregory P. Organic chemistry in colour. New York/Berlin/Heidelberg: Springer-Verlag; 1983.
[11] Pavlikova-Moricka M, Lacko I, Devinsky F, Masarova L, Mlynarcik D. Folia Microbiol 1994;39(3):176.
[12] Devinsky F, Kopecka-leitmanova A, Sersen F, Balgavy P. J Pharm Pharmcol 1990;42:790.
[13] Gregan F, Oremusova J, Remko M, Gregan J, Mlynarcik D. Il Farmaco 1998;53:41.
[14] Hugo WBJ. Appl Bact 1967;30(1):17.